

The electrochemical behaviour of ferrocene in deep eutectic solvents based on quaternary ammonium and phosphonium salts†

Cite this: *Phys. Chem. Chem. Phys.*, 2013, **15**, 1707

Laleh Bahadori,^a Ninie Suhana Abdul Manan,^b Mohammed Harun Chakrabarti,^{*ac} Mohd. Ali Hashim,^a Farouq Sabri Mjalli,^d Inas Muen AlNashef,^e Mohd. Azlan Hussain^a and Chee Tong John Low^f

The electrochemical behaviour of ferrocene (Fc) is investigated in six different deep eutectic solvents (DESS) formed by means of hydrogen bonding between selected ammonium and phosphonium salts with glycerol and ethylene glycol. Combinations of cyclic voltammetry and chronoamperometry are employed to characterise the DESS. The reductive and oxidative potential limits are reported *versus* the Fc/Fc⁺ couple. The diffusion coefficient, *D*, of ferrocene in all studied DESS is found to lie between 8.49×10^{-10} and 4.22×10^{-8} cm² s⁻¹ (these do not change significantly with concentration). The standard rate constant for heterogeneous electron transfer across the electrode/DESS interface is determined to be between 1.68×10^{-4} and 5.44×10^{-4} cm s⁻¹ using cyclic voltammetry. These results are of the same order of magnitude as those reported for other ionic liquids in the literature.

Received 3rd September 2012,
Accepted 3rd December 2012

DOI: 10.1039/c2cp43077k

www.rsc.org/pccp

1. Introduction

Recently, ionic liquids (ILs) as green reaction media have attracted some interest for a few industrial processes.^{1–3} ILs are composed entirely of ions and exist in the liquid state at temperatures below 100 °C. Their advantageous properties include negligible vapour pressure, good thermal and chemical stability, high polarity and non-flammability.^{4–7} In the area of electrochemistry, ILs may offer wide potential windows and intrinsic conductivity that abrogate the requirement for adding an extraneous supporting electrolyte. They also have good ion transport properties^{8–13} that have enabled their successful

applications in electrochemistry such as in electrochemical sensors,^{14,15} solar cells,¹⁶ fuel cells,¹⁷ electrochemical double-layer capacitors,¹⁸ lithium batteries^{19–21} and other solution based processes.^{22,23} Nevertheless, as the range of ILs expands, attention must be paid towards assuring that electrode potential data can be compared precisely with those acquired in conventional solvent–electrolyte media.

Although Katayama *et al.*²⁴ and Snook *et al.*²⁵ have shown that a credible Ag|Ag⁺ (IL) reference system is available, most electrochemical investigations of ILs have employed platinum,²⁶ or silver wire²⁷ quasi-reference electrodes, which can only give a qualitative impression of the reactions occurring between the interface of the electrode and the IL electrolyte.^{28–30}

In organic solvent media it is now routine to employ voltammetric data from IUPAC for arbitrarily selected and recommended compounds such as ferrocene, Fc, that display an exculpated, highly reversible redox process, as an ‘internal potential standard’. It is assumed that this redox couple is a nearly solvent-independent standard potential.³¹ Fc is widely used as an electrode transfer mediator for comparison of redox processes in different ILs.^{32–35} However, some studies show that the standard redox potential of Fc is dependent on solvation effects of the solvent and the supporting electrolyte used.^{36,37}

Despite such benefits of ILs, they have few industrial applications due to issues associated with high cost, purity and toxicity. Thus deep eutectic solvents (DESS) have been identified as

^a Department of Chemical Engineering, Faculty of Engineering, University of Malaya, Kuala Lumpur-50603, Malaysia. E-mail: mohammedharun77@yahoo.com

^b Department of Chemistry, Faculty of Science, University of Malaya, Kuala Lumpur 50603, Malaysia

^c Energy Futures Lab, Electrical Engineering Building, Imperial College London, South Kensington, London SW7 2AZ, UK

^d Petroleum & Chemical Engineering Department, Sultan Qaboos University, Muscat 123, Oman

^e Department of Chemical Engineering, College of Engineering, King Saud University, PO Box 800, Riyadh, Kingdom of Saudi Arabia

^f Electrochemical Engineering Laboratory, Energy Technology Research Group, Faculty of Engineering and the Environment, University of Southampton, Highfield, Southampton SO17 1BJ, UK

† Electronic supplementary information (ESI) available. See DOI: 10.1039/c2cp43077k

alternatives for ILs.^{38–40} They are basically formed by means of a mixture of metal halide bonds or hydrogen bonds along with that of the anion of a salt, as opposed to relying purely on electrostatic forces between anions and cations as in the case of ILs. DESs with various hydrogen bond donors have been demonstrated using acids, amides and alcohols.^{41,42} These liquids are easy to prepare in a pure state, they are non-reactive with water and most importantly they are biodegradable due to which, the toxicological properties of the components are well characterized.⁴² One of the biggest problems in reporting of DESs' properties is the wide difference between the melting point and fusion temperature, sometimes up to 125 °C.⁴¹ Thus, the possibility, indeed the reality, of alternative mechanistic pathways occurring in these solvents necessitates the development or modification of techniques capable of investigating reaction mechanisms in these media, and electrochemistry can contribute significantly to this.

DESs can be tailor made to suit different applications and the electrochemistry of Fc in two types of DESs prepared from choline chloride and trifluoroacetamide (TFA) or malonic acid as the hydrogen-bond donors was reported earlier.³⁹ But other kinds of DESs were not investigated in sufficient detail. In the current work we show how DESs formed by means of hydrogen bonding between two different ammonium and phosphonium salts with glycerin and ethylene glycol can be used as solvents for the electrochemical characterisation of Fc. We have used a combination of standard electrochemical techniques including cyclic voltammetry and chronoamperometry that may be considered to be sufficient for characterizing of the DESs. Based on the results obtained here, suitable DESs could be recommended for further experiments in the redox flow battery^{43–45} in future.

2. Experimental

2.1. Chemicals

Ferrocene ($\text{Fe}(\text{C}_5\text{H}_5)_2$, 98% purity) was purchased from Aldrich (USA). Choline chloride (ChCl) ($\text{C}_5\text{H}_{14}\text{ClNO}$), methyltriphenylphosphonium bromide ($\text{C}_{19}\text{H}_{18}\text{PBr}$), *N,N*-diethylethanol ammonium

chloride ($\text{C}_6\text{H}_{16}\text{ClNO}$), glycerol ($\text{C}_3\text{H}_8\text{O}_3$) and ethylene glycol ($\text{C}_2\text{H}_6\text{O}_2$) were purchased from Merck Chemicals (Germany) with high purity ($\geq 98\%$). All chemicals were used as supplied by the manufacturer and stored in an inert glove box purged with argon and the synthesized DESs were stored in tight capped bottles to prevent them from being affected by atmospheric humidity.

2.2. Synthesis of DESs

The original procedure for synthesising DESs as reported by Abbott and co-workers⁴⁰ was adapted in this work. A jacketed cup with a magnetic stirrer was used to mix both the salt and hydrogen-bond donor at 353.15 K and atmospheric pressure for a period of 3 hours (at a minimum) until a homogeneous colourless liquid was formed. The synthesis experiments were conducted in a glove box with firm humidity control of less than 1 ppm water. Fig. 1 shows the structures of the salts and hydrogen bond donors that make up the DESs chosen for this study and Table 1 indicates their physical properties.

2.3. Characterization of DESs

Freezing temperatures of the synthesized DESs were measured using a Mettler Toledo Differential Scanning Calorimetry (DSC) device and the viscosities of the DESs were measured using a Haake VT550 instrument. The equipment was calibrated with standard values of freezing points and viscosities of samples of pure water and glycerol. The conductivities were measured using a DZS-708 Multi-parameter Analyser. The conductivity meter was calibrated using a 0.001 mol L⁻¹ standard solution of KCl (Merck).

2.4. Electrochemical set-up

The electrochemical cell consisted of a typical three-electrode set-up. The counter electrode was a Pt wire, and an Ag wire (immersed in 65% HNO_3 prior to experiments, then rinsed thoroughly with water and ethanol) was used as a quasi-reference electrode. A platinum microelectrode (20 μm diameter) and

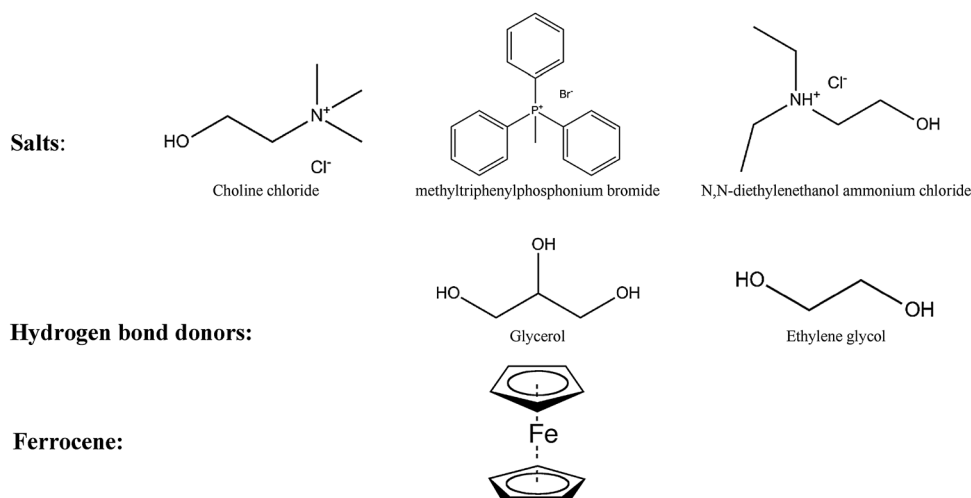


Fig. 1 Structures of all the salts and hydrogen bond donors used in this study and the species under investigation.

Table 1 Physical properties of the different DESs synthesized in this study

Salt	Hydrogen-bond donor	Molar ratio (salt : HBD)	Abbreviation	Melting point (K)	Conductivity (mS cm ⁻¹)	Viscosity (mPa s)
Methyltriphenylphosphonium bromide	Ethylene glycol	1 : 2	DES1	230	1.43	213
Methyltriphenylphosphonium bromide	Glycerol	1 : 3	DES2	267	0.08	3040
Choline chloride	Ethylene glycol	1 : 2	DES3	207	5.26	66
Choline chloride	Glycerol	1 : 2	DES4	237	0.65	322
<i>N,N</i> -Diethylethanol ammonium chloride	Ethylene glycol	1 : 2	DES5	242	5.72	58
<i>N,N</i> -Diethylethanol ammonium chloride	Glycerol	1 : 2	DES6	267	0.25	577

Glassy Carbon (GC, 3 mm diameter) were used as working electrodes. The working electrodes were carefully polished before each voltammetry experiment with 0.25 μm alumina suspension and ultrasonically rinsed in acetone. All electrochemical experiments were performed using a computer-controlled *i*-Autolab potentiostat (PGSTAT302N) and the electrochemical cell was assembled at room temperature within a Faraday cage, which in turn was situated inside the dry argon-filled glove box. Humidity levels were measured continuously to ensure that the total moisture content inside the glove box never exceeded 1 wt%.

2.5. Chronoamperometric experiments

Potential step chronoamperometric transients were achieved using a sample time of 0.01 s. The pre-treatment step comprised of holding the potential at a point of zero current (with 20 s pre equilibration time), after which the potential was stepped from a position of zero current to a chosen potential after the oxidative peak and the current was measured for 10 s. The nonlinear curve fitting function in the software package Origin 6.0 (Microcal Software Inc.), following the Shoup and Szabo⁴⁶ approximation (eqn (1)–(3)) as employed previously,^{27,46} was used to fit the experimental data.

$$I = -4nFDcr_d f(\tau) \quad (1)$$

$$f(\tau) = 0.7854 + 0.8863\tau^{-1/2} + 0.2146\exp(-0.7823\tau^{-1/2}) \quad (2)$$

$$\tau = \frac{4Dt}{r_d^2} \quad (3)$$

where n is the number of electrons transferred, F is Faraday's constant, D is the diffusion coefficient, c is the bulk concentration of the electroactive species, r_d is the radius of the microdisk electrode, and t is the time. The software was instructed to perform one hundred iterations on the data, stopping when the experimental data have been optimized. A value for the diffusion coefficient, D , and the product of the number of electrons and the concentration of the electroactive species, nc , were obtained after optimization of the experimental data.

3. Results and discussion

3.1. Cyclic voltammetry for oxidation of Fc in various DESs

It is essential to employ either a reference electrode with a familiar potential against a standard hydrogen electrode or

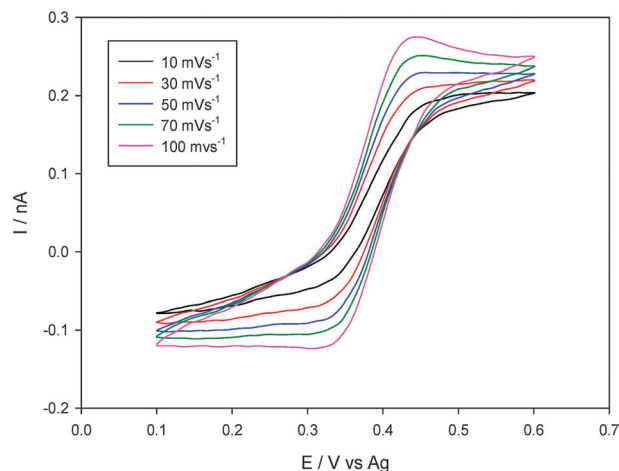


Fig. 2 Cyclic voltammogram for the oxidation of 5.21 mM Fc in DES5 on a Pt electrode (diameter 20 μm) at varying scan rates of 10, 30, 50, 70 and 100 mV s^{-1} (from bottom to top).

refer all data to a procedure whose reversible potential has to be independent of the DESs, in order to compare voltammetric data from different eutectic solvents. The ferrocene/ferrocenium ($\text{Fc}^{0/+}$) couple is most prevalently used as an internal potential scale standard in voltammetry in conventional organic solvent media.^{31,47} This process is also used in IL electrochemistry.³⁰ Fig. 2 shows typical cyclic voltammograms for the oxidation of 5.21 mM solution of Fc in DES5 on a platinum microelectrode (20 μm diameter) at scan rates ranging from 10 to 100 mV s^{-1} (the remaining figures for Fc in the other five DESs investigated are shown in Fig. S1, ESI[†]). The voltammetry is reported against a silver wire quasi-reference electrode and a Pt counter electrode. The scan rate dependence indicates that the oxidation of Fc to Fc^+ in DESs follows eqn (4).



The quantitative relationship of data obtained from conventional voltammetric experiments on DESs such as values of the reversible half wave potential ($E_{1/2}$) calculated as the average of anodic and cathodic peak potentials ($(E_{\text{pa}} + E_{\text{pc}})/2$), the peak-to-peak potential separation ($\Delta E_p = E_{\text{pa}} - E_{\text{pc}}$), the ratio of the peak current of oxidation and reduction components ($i_{\text{pa}}/i_{\text{pc}}$) and the peak width at half-height ($W_{1/2}$) for both oxidation and reduction

Table 2 Cyclic voltammetric data for oxidation of ferrocene in DESs

DESs	ν (V s ⁻¹)	i_{pa}/i_{pc}	ΔE_p (mV)	$E_{1/2}$ (mV)	$W_{1/2}$ (mV)	
					Oxidized species	Reduced species
DES1	0.01	1.12	91	386	147	171
	0.05	1.08	91	388	142	178
	0.07	1.02	91	388	150	176
	0.1	0.98	91	386	153	171
	0.5	0.99	91	386	149	169
	1	0.97	93	386	150	170
DES2	0.01	0.98	70	381	136	117
	0.05	1.02	71	379	139	140
	0.07	1	73	379	144	155
	0.1	0.96	73	383	145	139
	0.5	0.98	80	381	145	158
	1	1.08	80	380	149	148
DES3	0.01	1.06	100	372	138	127
	0.05	1	101	375	159	159
	0.07	1.15	101	376	149	173
	0.1	1.02	103	373	156	158
	0.5	1.2	106	372	155	177
	1	1.24	110	372	163	172
DES4	0.01	1.22	80	352	138	145
	0.05	1.05	80	353	148	122
	0.07	1	80	352	155	153
	0.1	1.02	85	352	152	161
	0.5	1.02	95	356	158	177
	1	1.2	96	353	155	149
DES5	0.01	0.99	89	389	142	168
	0.05	1.05	89	388	140	148
	0.07	1	89	389	141	155
	0.1	0.98	89	387	139	143
	0.5	1.05	92	394	141	138
	1	0.97	100	398	142	151
DES6	0.01	1	78	372	140	152
	0.05	1.06	79	377	141	150
	0.07	0.98	81	375	140	149
	0.1	0.96	88	372	143	151
	0.5	1	92	376	139	148
	1	0.98	98	377	140	152

Table 3 Electrochemical potential windows obtained at GC and Pt working electrodes for the DESs studied in this work

DESs	Electrode materials	Anodic limit (V)	Cathodic limit (V)	Potential windows (V)
DES1	GC	0.71	-1.72	2.43
	Pt	0.68	-1.04	1.72
DES2	GC	0.78	-1.81	2.59
	Pt	0.78	-1.10	1.88
DES3	GC	1.20	-2.29	3.49
	Pt	1.18	-1.21	2.39
DES4	GC	1.31	-2.19	3.50
	Pt	1.28	-1.18	2.46
DES5	GC	1.26	-2.22	3.48
	Pt	1.18	-0.85	2.03
DES6	GC	1.32	-2.20	3.52
	Pt	1.21	-0.80	2.01

DESs was attributed to the presence of uncompensated solution resistance.⁴⁸ Also it was observed that for different scan rates $E_{1/2}$ and $W_{1/2}$ remained constant. The redox potential for a couple was better approximated by the half-wave potential ($E_{1/2}$) rather than by the cathodic peak (E_{pc}) or anodic peak (E_{pa}) potential, because both E_{pa} and E_{pc} change with the scan rates while $E_{1/2}$ is independent of the scan rate; as was expected for a reversible system. It was found that $E_{1/2}$ shifts toward more positive potential conforming to the following order: DES5 > DES1 > DES2 > DES6 \geq DES3 > DES4. This order reveals that the oxidation of ferrocene to ferrocenium becomes more difficult on going from DES4 to DES5. The overall $E_{1/2}$ difference between DES5 and DES4 was found to be around 45 mV.

In consideration of the above, we assumed that the electrochemical reaction of $[Fc]/[Fc^+]$ was reversible at the respective scan rates in order to calculate the diffusion coefficients of Fc and Fc^+ . The peak current linearly varies with the square root of the scan rate on a platinum microelectrode as shown in Fig. 3

processes is shown in Table 2. In addition, the potential windows for all DESs have been measured by cyclic voltammetry at a scan rate of 100 mV s⁻¹ using GC or Pt as the working electrode. The reduction and oxidation potential limits are also summarized in Table 3. It was observed that DESs made up of ammonium salts gave a larger potential window in comparison with the phosphonium based ones when GC was used as the working electrode. This potential window decreased when GC was replaced with Pt.

In all investigated DESs, the cathodic and anodic peak currents increased with increasing scan rate and the peak current ratio of the reverse and the forward scans was close to unity ($i_{pa}/i_{pc} = 1.0$) and was independent of the scan rate. The peak-to-peak potential separation (ΔE_p) in the cyclic voltammograms at different scan rates was estimated to be in the range of 0.07–0.1 V. A fast, reversible, one-electron transfer would ideally have a $\Delta E_p = 0.059$ V at 298 K. The discrepancy from this ideal value at higher concentrations and scan rates in

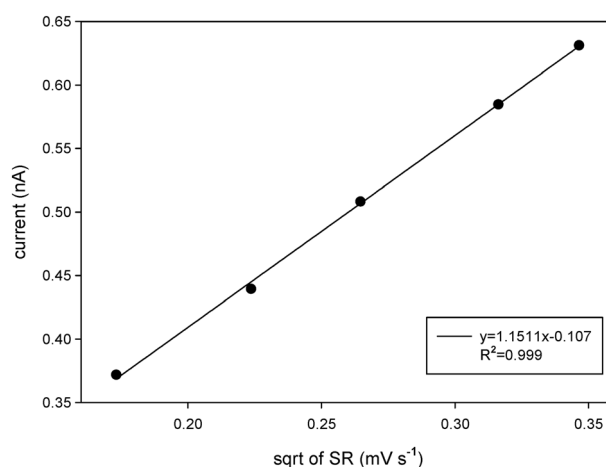
**Fig. 3** Linear dependence of peak current vs. square root of scan rates for Fc/Fc⁺ using a Pt electrode in different DESs. Plot for 5.21 mM solution of Fc in DES5 is clearly shown.

Table 4 Concentration-dependent diffusion coefficients of Fc in DESs solution

DESs	Concentration (mM)	D_{CV}^a (cm ² s ⁻¹)	D_{CA}^b (cm ² s ⁻¹)
DES1	1.08	4.54×10^{-9} (± 0.08)	4.30×10^{-9} (± 0.05)
	5.21	4.32×10^{-9} (± 0.10)	4.21×10^{-9} (± 0.03)
	10.13	4.56×10^{-9} (± 0.06)	3.86×10^{-9} (± 0.08)
	20.18	4.23×10^{-9} (± 0.04)	4.33×10^{-9} (± 0.06)
	30.06	4.02×10^{-9} (± 0.08)	4.36×10^{-9} (± 0.08)
DES2	1.08	9.42×10^{-10} (± 0.07)	8.65×10^{-10} (± 0.04)
	5.21	8.96×10^{-10} (± 0.05)	8.96×10^{-10} (± 0.05)
	10.13	9.12×10^{-10} (± 0.06)	8.88×10^{-10} (± 0.05)
	20.18	9.03×10^{-10} (± 0.08)	8.62×10^{-10} (± 0.03)
	30.06	9.86×10^{-10} (± 0.06)	8.49×10^{-10} (± 0.10)
DES3	1.08	2.94×10^{-8} (± 0.06)	3.46×10^{-8} (± 0.06)
	5.21	3.11×10^{-8} (± 0.10)	3.32×10^{-8} (± 0.05)
	10.13	3.08×10^{-8} (± 0.09)	3.12×10^{-8} (± 0.04)
	20.18	3.22×10^{-8} (± 0.08)	3.39×10^{-8} (± 0.08)
	30.06	3.19×10^{-8} (± 0.04)	2.98×10^{-8} (± 0.08)
DES4	1.08	4.01×10^{-9} (± 0.09)	3.82×10^{-9} (± 0.10)
	5.21	3.90×10^{-9} (± 0.10)	4.13×10^{-9} (± 0.10)
	10.13	4.07×10^{-9} (± 0.08)	3.96×10^{-9} (± 0.09)
	20.18	3.96×10^{-9} (± 0.04)	4.12×10^{-9} (± 0.05)
	30.06	3.86×10^{-9} (± 0.07)	4.08×10^{-9} (± 0.05)
DES5	1.08	2.98×10^{-8} (± 0.08)	4.01×10^{-8} (± 0.03)
	5.21	3.20×10^{-8} (± 0.05)	4.22×10^{-8} (± 0.04)
	10.13	3.22×10^{-8} (± 0.10)	3.95×10^{-8} (± 0.02)
	20.18	3.26×10^{-8} (± 0.06)	4.16×10^{-8} (± 0.02)
	30.06	3.25×10^{-8} (± 0.08)	3.89×10^{-8} (± 0.08)
DES6	1.08	2.80×10^{-9} (± 0.08)	3.65×10^{-9} (± 0.06)
	5.21	3.08×10^{-9} (± 0.09)	3.55×10^{-9} (± 0.08)
	10.13	3.25×10^{-9} (± 0.03)	3.40×10^{-9} (± 0.04)
	20.18	2.97×10^{-9} (± 0.08)	3.86×10^{-9} (± 0.04)
	30.06	3.02×10^{-9} (± 0.09)	3.93×10^{-9} (± 0.03)

^a D_{Fc} values were determined using cyclic voltammetry. ^b D_{Fc} values were determined using chronoamperometry. Temperature 298 ± 1 K. Error bars are calculated from the standard deviation from four experimental repetitions.

(the remaining plots for Fc in the other five DESs investigated are shown in Fig. S2, ESI†). This confirms that the process is mainly regulated by the diffusion of Fc/Fc⁺ in the DESs.

The diffusion coefficients (D) have been calculated using the Randles-Sevcik equation (eqn (5)),^{49,50} which presumes that mass transport occurs only by a diffusion process and they are given in Table 4. According to the Randles-Sevcik equation, i_{pa} and i_{pc} are proportional to $\nu^{1/2}$ and hence a plot of i_{pa} or i_{pc} versus $\nu^{1/2}$ gives a straight line, the slope of which can be used to determine the diffusion coefficient.

$$i_p = 0.4463(nF)^{3/2}(RT)^{-1/2}AD^{1/2}C_0\nu^{1/2} \quad (5)$$

where i_p is the peak current (A), n is the number of electron equivalents exchanged during the redox process (electron stoichiometry), A is the electrode area (cm²), D is the diffusion coefficient of the electroactive species (cm² s⁻¹), ν is the voltage scan rate (V s⁻¹), C_0 is the bulk concentration of the electroactive species (mol cm⁻³), R is the universal gas constant, T is the absolute temperature (K) and F is Faraday's constant.

3.2. Chronoamperometric transients of Fc^{0/+} in DESs

Potential step simulation was first applied to the aqueous one-electron oxidation of Fc to Fc⁺ since the diffusion coefficients of both species are well established in the literature.⁵¹ Potential step chronoamperometry was conducted using a platinum microelectrode immersed in solutions of Fc in DESs at various concentrations in order to calculate diffusion coefficients of Fc. The potential was stepped from 0 V where no Faradaic reaction occurred to +0.6 V (corresponding to the oxidation of Fc to Fc⁺) and the transient procured is exhibited in Fig. 4 (the remaining figures for Fc in the other five DESs investigated are shown in Fig. S3, ESI†). The diffusion coefficient, D , of Fc has been determined using the Cottrell equation (eqn (6)). The experimental plots of i versus $t^{-1/2}$ with the best fits at an intercept of zero for different concentrations of Fc were employed.

$$i_p = nFACD^{1/2}\pi^{-1/2}t^{-1/2} \quad (6)$$

In this equation, n is the number of electrons, A is the electrode area (cm²), F is Faraday's constant, t is the time (s) and C is the bulk concentration (mol cm⁻³).

To further support this conclusion and analyse these transients, the data obtained from the first potential step were initially fitted to the analytical Shoup and Szabo expression⁴⁶ in order to determine the diffusion coefficient for Fc after inputting values for the concentration and the electrode radius. A close fit between the experimental and simulated transients of Fc/Fc⁺ was achieved, as shown for a typical experimental transient in Fig. 4. It indicated that the oxidation process was diffusion controlled. The values for D_{Fc} using the chronoamperometry technique are displayed in Table 4. Herein, D_{Fc} were found to be lower than those determined in organic solvents due to lower viscosities.⁵² However, the diffusion coefficients of Fc reported here are of the same order of magnitude as those of ILs.^{11,32}

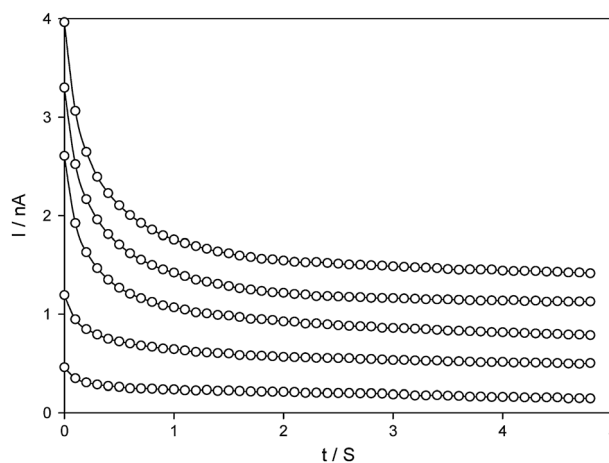


Fig. 4 Experimental (—) and fitted theoretical (○) chronoamperometric transients for the oxidation of 1.08, 5.21, 10.13, 20.18 and 30.06 mM Fc in DESs on a 20 μm Pt microelectrode.

3.3. The heterogeneous electron-transfer rates for the oxidation of ferrocene in DESs

Nicholson's method⁵³ was the first approach used to evaluate the heterogeneous rate constant (k_s). Anodic and cathodic peak separations from a background were subtracted from a voltammogram of a simple one electron transfer reaction and further used to determine ψ from which k_s was achieved using eqn (7):

$$\psi = \frac{k_s}{(\pi a D_0)^{1/2}} \quad (7)$$

where $a = nF\nu/RT$, D_0 is the diffusion coefficient, ν is the scan rate and all other symbols have their usual meaning. For this experiment the data have been acquired at 298.15 K, $C = 5.21$ mM, and $\nu = 0.1$ V s⁻¹ and thus linear diffusion was expected to dominate. If diffusion coefficients have been determined, either from cyclic voltammetry for a fully reversible system or using a suitable chronoamperometric technique, k_s can be estimated by measuring cyclic voltammograms at various scan rates and fitting the observed variation in peak separation to tabulated values. The values of the heterogeneous rate constant were determined to be 1.72×10^{-4} (± 0.03), 2.09×10^{-4} (± 0.02), 3.08×10^{-4} (± 0.06), 2.18×10^{-4} (± 0.03), 5.44×10^{-4} (± 0.02) and 1.68×10^{-4} cm s⁻¹ (± 0.07), respectively, in DES1 to DES6. From the comparison of k_s , it can be inferred that the rate constants of ammonium based DESs were greater than those of phosphonium based ones.

3.4. Viscosity dependence of diffusion coefficient

The mass transport properties of a spherical species can be predicted using the Stokes–Einstein equation (8), which relates the diffusion coefficient of the species, D , and the dynamic viscosity of the medium, η . Here k_B is the Boltzmann constant, α is the hydrodynamic radius of the species, and T is the absolute temperature.

$$D = \frac{k_B T}{6\pi\eta\alpha} \quad (8)$$

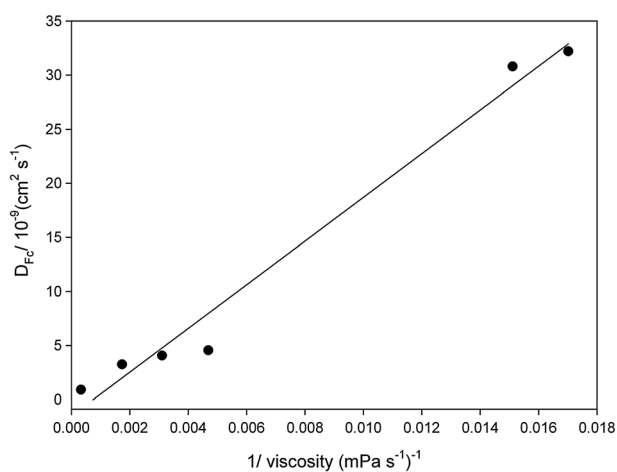


Fig. 5 Plot of diffusion coefficient (D) against the inverse of viscosity (η^{-1}) for the six DESs studied. D values were obtained from cyclic voltammetry analysis at concentrations of 10.13 mM.

According to eqn (8), a plot of D vs. η^{-1} should be linear with zero intercept. Fig. 5 exhibits linear behaviour when D_{Fc} is plotted vs. η^{-1} for 10.13 mM ferrocene in six different DESs. Thus, it might be sensible to presume that the Stokes–Einstein relationship, as shown in eqn (8), applied to the data reported herein. Furthermore, many reports in the literature indicated that the Stokes–Einstein equation applies for a range of redox species in various ILs (inclusive of ferrocene), as indicated by linear plots of D vs. η^{-1} .^{32,53} However, there are other reports that eqn (8) does not apply in ILs, particularly when the redox species is small in size.⁵⁴ The largest D_{Fc} value was measured in DES5 which is the least viscous DES, and it was approximately 30 times larger than the diffusion coefficient measured in DES3.

3.5. Concentration dependence of diffusion coefficient

Data obtained for D_{Fc} from both cyclic voltammetry and chronoamperometry at various concentrations are presented in Table 4. Fig. 4 shows potential step chronoamperometry for the oxidation of Fc at concentrations of 1.08, 5.21, 10.13, 20.18 and 30.06 mM in DESs on a 20 μ m diameter platinum electrode. The potential was stepped from 0.0 V (no Faradaic current) to 0.6 V vs. Ag wire to oxidize the Fc to Fc⁺. The experimental data (—) fit the simulation data (○) well, referring to the fitting procedure indicated in the Experimental section. The remaining figures for Fc in the other five DESs investigated are shown in Fig. S3 (ESI[†]). Typical cyclic voltammetry was undertaken at a range of concentrations of Fc in DESs to determine diffusion coefficients for Fc as a function of concentration. As expected, the peak current due to Fc oxidation increased with increasing concentration. However, the diffusion coefficient of Fc did not change considerably. As can be seen, the ratio of the diffusion coefficients from both experimental techniques remained constant throughout the whole concentration range assuming that the diffusion was independent of the concentration in DESs.

4. Conclusions

The electrochemical oxidation of Fc has been studied by cyclic voltammetry and potential step chronoamperometry in 6 different DESs formed by means of hydrogen bonding between two different ammonium and phosphonium salts with glycerin and ethylene glycol. The potential windows of DESs have been determined electrochemically at a Pt microelectrode and a GC electrode. The reductive and oxidative potential limits have been reported versus the Fc/Fc⁺ couple. It is observed that DESs made up of ammonium salts give a larger potential window compared with the phosphonium based ones when either Pt or GC working electrode is employed. Results show that D for Fc does not change significantly with concentration in both techniques. Fc/Fc⁺ complies with classical Stokes–Einstein behaviour in terms of the D vs. η^{-1} dependence. The kinetics of electron transfer across the DES/electrode interface have been studied using cyclic voltammetry and the highest standard heterogeneous rate constant is determined to be 5.44×10^{-4} cm s⁻¹ in the ammonium based DES prepared from *N,N*-diethylethanol ammonium chloride and ethylene

glycol (DES5). It would be interesting to perform battery charge-discharge experiments of vanadium acetylacetonate in DES5 for future work.

Acknowledgements

The authors are grateful to the High Impact Research Grant (UM.C/HIR/MOHE/ENG/18) provided by the University of Malaya and the Ministry of Higher Education in Malaysia as well as to the Deanship of Scientific Research at King Saud University, Saudi Arabia (RGP-VPP-108), which enabled this research work to be carried out successfully. MHC shows special gratitude to Professor N. P. Brandon for allowing full access to experimental facilities in Imperial College London.

References

- 1 K. Shahbaz, F. S. Mjalli, M. A. Hashim and I. M. AlNashef, *Energy Fuels*, 2011, **25**, 2671.
- 2 W. Wei, H. H. Jin and G. C. Zhao, *Microchim. Acta*, 2009, **164**, 167.
- 3 M. Hayyan, F. S. Mjalli, M. A. Hashim, I. M. AlNashef, S. M. Al-Zahrani and K. L. Chooi, *J. Electroanal. Chem.*, 2012, **664**, 26.
- 4 I. M. AlNashef, M. L. Leonard, M. C. Kittle, M. A. Matthews and J. W. Weidner, *Electrochem. Solid-State Lett.*, 2001, **4**, D16.
- 5 P. Earis, *Analyst*, 2005, **130**, T11.
- 6 A. P. Abbott, G. Capper, B. G. Swain and D. A. Wheeler, *Trans. Inst. Met. Finish.*, 2005, **83**, 51.
- 7 F. Endres and S. Z. El Abedin, *Phys. Chem. Chem. Phys.*, 2006, **8**, 2101.
- 8 O. Höfft and F. Endres, *Phys. Chem. Chem. Phys.*, 2011, **13**, 13472.
- 9 M. Galinski, A. Lewandowski and I. Stepniak, *Electrochim. Acta*, 2006, **51**, 5567.
- 10 B. K. Sweeny and D. G. Peters, *Electrochem. Commun.*, 2001, **3**, 712.
- 11 C. Zhao, G. Burrell, A. A. J. Torriero, F. Separovic, N. F. Dunlop, D. R. MacFarlane and A. M. Bond, *J. Phys. Chem. B*, 2008, **112**, 6923.
- 12 M. Deepa, A. Awadhia and S. Bhandari, *Phys. Chem. Chem. Phys.*, 2009, **11**, 5674.
- 13 A. P. Doherty and C. A. Brooks, *Electrochim. Acta*, 2004, **49**, 3821.
- 14 B. Li, L. Wang, B. Kang, P. Wang and Y. Qiu, *Sol. Energy Mater. Sol. Cells*, 2006, **90**, 549.
- 15 W. Wei, H.-H. Jin and G.-C. Zhao, *Microchim. Acta*, 2009, **164**, 167.
- 16 E. Guillén, J. Idígoras, T. Berger, J. A. Anta, C. Fernández-Lorenzo, R. Alcántara, J. Navas and J. Martín-Calleja, *Phys. Chem. Chem. Phys.*, 2011, **13**, 207.
- 17 E. R. Choban, J. S. Spendelow, L. Gancs, A. Wieckowski and P. J. A. Kenis, *Electrochim. Acta*, 2005, **50**, 5390.
- 18 L. Timperman, P. Skowron, A. Boisset, H. Galiano, D. Lemordant, E. Frackowiak, F. Béguin and M. Anouti, *Phys. Chem. Chem. Phys.*, 2012, **14**, 8199.
- 19 S.-L. Chou, J.-Z. Wang, J.-Z. Sun, D. Wexler, M. Forsyth, H.-K. Liu, D. R. MacFarlane and S.-X. Dou, *Chem. Mater.*, 2008, **20**, 7044.
- 20 A. Fericola, B. Scrosati and H. Ohno, *Ionics*, 2006, **12**, 95.
- 21 D. R. MacFarlane, J. M. Pringle, P. C. Howlett and M. Forsyth, *Phys. Chem. Chem. Phys.*, 2010, **12**, 1659.
- 22 V. I. Parvulescu and C. Hardacre, *ChemInform*, 2007, **107**, 2616.
- 23 N. V. Plechkova and K. R. Seddon, *Chem. Soc. Rev.*, 2008, **37**, 123.
- 24 Y. Katayama, S. Dan, T. Miura and T. Kishi, *J. Electrochem. Soc.*, 2001, **148**, C102.
- 25 G. A. Snook, A. S. Best, A. G. Pandolfo and A. F. Hollenkamp, *Electrochem. Commun.*, 2006, **8**, 1405.
- 26 P. A. Z. Suarez, V. M. Selbach, J. E. L. Dullius, S. Einloft, C. M. S. Piatnicki, D. S. Azambuja, R. F. de Souza and J. Dupont, *Electrochim. Acta*, 1997, **42**, 2533.
- 27 R. G. Evans, O. V. Klymenko, C. Hardacre, K. R. Seddon and R. G. Compton, *J. Electroanal. Chem.*, 2003, **556**, 179.
- 28 V. M. Hultgren, A. W. Mariotti, A. M. Bond and A. G. Wedd, *Anal. Chem.*, 2002, **74**, 3151.
- 29 J. Zhang and A. M. Bond, *Anal. Chem.*, 2003, **75**, 2694.
- 30 J. Zhang and A. M. Bond, *Analyst*, 2005, **130**, 1132.
- 31 G. Gritzner and J. Kuta, *Electrochim. Acta*, 1984, **29**, 869.
- 32 E. I. Rogers, D. S. Silvester, D. L. Poole, L. Aldous, C. Hardacre and R. G. Compton, *J. Phys. Chem. C*, 2008, **112**, 2729.
- 33 J. E. F. Weaver, D. Breadner, F. Deng, B. Ramjee, P. J. Ragona and R. W. Murray, *J. Phys. Chem. C*, 2011, **115**, 19379.
- 34 L. E. Barrosse-Antle, C. Hardacre and R. G. Compton, *J. Phys. Chem. B*, 2009, **113**, 2805.
- 35 A. Lewandowski, L. Waligora and M. Galinski, *Electroanalysis*, 2009, **21**, 2221.
- 36 A. A. J. Torriero, J. Sunarso and P. C. Howlett, *Electrochim. Acta*, 2012, **82**, 60.
- 37 A. A. J. Torriero and P. C. Howlett, *Electrochem. Commun.*, 2012, **16**, 84.
- 38 A. P. Abbott, K. El Ttaib, G. Frisch, K. J. McKenzie and K. S. Ryder, *Phys. Chem. Chem. Phys.*, 2009, **11**, 4269.
- 39 C. A. Nkuku and R. J. LeSuer, *J. Phys. Chem. B*, 2007, **111**, 13271.
- 40 A. P. Abbott, D. Boothby, G. Capper, D. L. Davies and R. K. Rasheed, *J. Am. Chem. Soc.*, 2004, **126**, 9142.
- 41 A. P. Abbott and K. J. McKenzie, *Phys. Chem. Chem. Phys.*, 2006, **8**, 4265.
- 42 A. P. Abbott, G. Capper, K. J. McKenzie and K. S. Ryder, *J. Electroanal. Chem.*, 2007, **599**, 288.
- 43 M. H. Chakrabarti, R. A. W. Dryfe and E. P. L. Roberts, *Electrochim. Acta*, 2007, **52**, 2189.
- 44 M. H. Chakrabarti, R. A. W. Dryfe and E. P. L. Roberts, *J. Chem. Soc. Pak.*, 2007, **29**, 294.

- 45 M. H. Chakrabarti and E. P. L. Roberts, *NED Univ. J. Res.*, 2008, **5**, 43.
- 46 D. Shoup and A. Szabo, *J. Electroanal. Chem. Interfacial Electrochem.*, 1982, **140**, 237.
- 47 A. M. Bond, K. B. Oldham and G. A. Snook, *Anal. Chem.*, 2000, **72**, 3492.
- 48 J. E. B. Randles, *Trans. Faraday Soc.*, 1948, **44**, 327.
- 49 C. M. Comminges, R. Barhdadi, M. Laurent and M. Troupel, *J. Chem. Eng. Data*, 2006, **51**, 680.
- 50 R. N. Adams, *Electrochemistry at Solid Electrodes*, Marcel Dekker, New York, 1969.
- 51 A. A. J. Torriero, A. I. Siriwardana, A. M. Bond, I. M. Bugar, N. F. Dunlop, G. B. Deacon and D. R. MacFarlane, *J. Phys. Chem. B*, 2009, **113**, 11222.
- 52 N. Tsierkezos, *J. Solution Chem.*, 2007, **36**, 289.
- 53 R. S. Nicholson, *Anal. Chem.*, 1965, **37**, 1351.
- 54 X.-J. Huang, E. I. Rogers, C. Hardacre and R. G. Compton, *J. Phys. Chem. B*, 2009, **113**, 8953.